Nat Hazards (2015) 78:583–602
DOI 10.1007/s11069-015-1734-6

ORIGINAL PAPER

Seismic risk assessment and hazard mapping in Nepal

Hemchandra Chaulagain[1,2] · Hugo Rodrigues[3] · Vitor Silva[1] · Enrico Spacone[4] · Humberto Varum[5]

Received: 19 June 2014 / Accepted: 31 March 2015 / Published online: 12 April 2015
© Springer Science+Business Media Dordrecht 2015

Abstract Seismic risk in the form of impending disaster has been seen from past records that moderate-to-large earthquakes have caused the loss of life and property in all parts of Nepal. Despite the availability of new data, and methodological improvements, the available seismic hazard map of Nepal is about two decades old. So an updated seismic hazard model at the country level is imperative and logical. The seismic hazard and risk model constitute important tools for framing public policies toward land-use planning, building regulations, insurance, and emergency preparedness. In fact, the reliable estimation of seismic hazard and risk eventually minimizes social and economic disruption caused by earthquakes. In this frame of reference, the seismic risk assessment at a country level is elementary in reducing potential losses stemming from future earthquakes. Thus, this study investigates structural vulnerability, seismic risk, and the resulting possible economic losses owing to future earthquakes in Nepal. To this end, seismic risk assessment in Nepal is done using an existing probabilistic seismic hazard, a newly developed structural vulnerability, and recently released exposure data. The OpenQuake-engine, the open-source platform for seismic hazard and risk assessment from the Global Earthquake Model initiative, was used to calculate the seismic hazard and risk in Nepal. The seismic hazard and mean economic loss map were formulated for the 1, 2, 5, and 10 % probability of exceedance in 50 years. Finally, the distribution of building damage and corresponding economic losses due to the recurrence of the historical 1934 earthquake was presented in this study.

✉ Hugo Rodrigues
hugo.f.rodrigues@ipleiria.pt

1 Civil Engineering Department, University of Aveiro, 3810-193 Aveiro, Portugal

2 Civil Engineering Department, Oxford College of Engineering and Management, Gaidakot, Nawalparashi, Nepal

3 School of Technology and Management, Polytechnic Institute of Leiria, 2411-901 Leiria, Portugal

4 Department PRICOS – Architettura, University of Chieti-Pescara, 65127 Pescara, Italy

5 Department of Civil Engineering, Faculty of Engineering of the University of Porto, 4200-465 Porto, Portugal

Keywords Nepalese buildings · Structural vulnerability · Seismic hazard · Seismic risk

1 Introduction

Nepal is situated in the Himalayan region. Geologically, the Himalayan region is divided into higher Himalaya, sub-Himalaya, lesser Himalaya, and Tethyan Himalaya. There are four major structural units in the Himalaya: (a) the Main Frontal Thrust (MFT); (b) the Main Boundary Thrust (MBT); (c) the Main Central Thrust (MCT); and (d) the South Tibet Detachment (STD). The Main Frontal Thrust lies between the sediments of the Indo-Gangetic Plains and outer Himalaya. The border between outer and lesser Himalaya; and lesser and higher Himalaya are known as MBT and MCT, respectively. The South Tibetan Detachment (STD) lies between the higher and Tethys Himalaya. The location of MFT, MBT, MCT, and STD is presented in Fig. 1. Among these, active faults along the MBT and MFT are the most active and have potential to produce large earthquakes in the future (Lava and Avouac 2000).

The active faults in and around the Himalayan belt are direct indicators of recent crustal movement as a result of the collision between the Indian and Eurasian plates. Several major earthquakes were reported in 1255, 1810, 1866, 1934, 1980, and 1988 in Nepal (Pandey et al. 1995). Among the major earthquakes recorded in history, the great Bihar–Nepal earthquake of 1934, with a maximum intensity of X (MMI), caused extensive damage in the eastern half of Nepal and resulted in more than 8500 deaths. In addition, about 19 % of the buildings were completely destroyed and 38 % of the buildings were badly damaged (Rana 1935). More recently, the earthquake of August 21, 1988, with a magnitude 6.6 (M_w), stroked the eastern part of Nepal and killed 721 people, injured 6553, and damaged or collapsed 66,541 buildings (Thapa 1988).

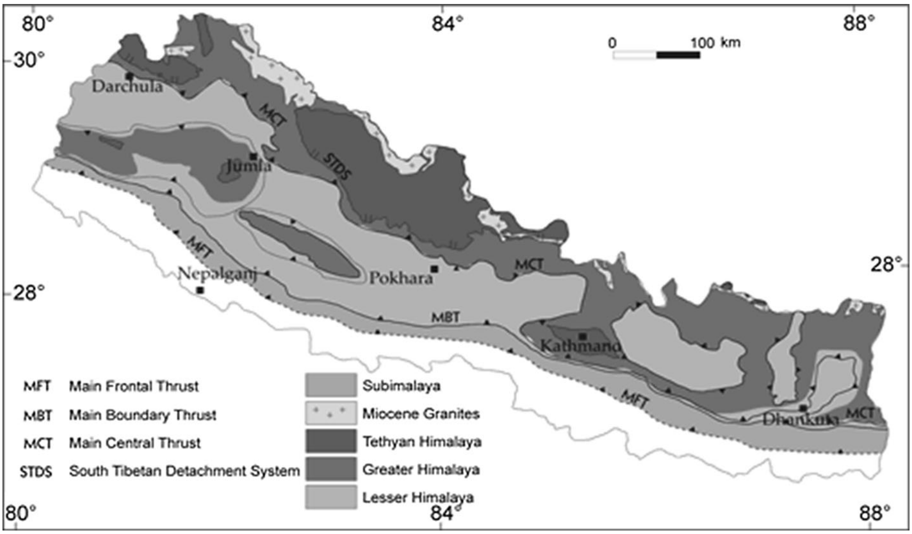

Fig. 1 Geological map of Nepal (adapted from Upreti 1999)

Despite this worrying scenario, the previous research works conducted by the National Society for Earthquake Technology, Nepal (NSET 2001), and the Japan International Cooperation Agency (JICA 2002) expected that 50 % of the buildings would be damaged and 1.3 % of the population would perish for a large earthquake with a magnitude 8 (M_w) occurred 100 km east from the Kathmandu Valley. Afterwards, Wyss (2005) calculated the expected fatalities and injuries in the western part of Nepal. He estimated a minimum death toll of about 15,000 in sparsely populated areas and a maximum of about 150,000 death toll in a populous area for an earthquake of magnitude 8.1 (M_w). The number of injuries was expected to range from 40,000 to 250,000. Owing to the poor socioeconomic and uncontrolled building construction, a developing country such as Nepal typically suffers far greater losses from earthquakes than developed countries (Wyss et al. 2012).

In these circumstances, this study tries to explore seismic risk in Nepal by combining probabilistic seismic hazard, structural vulnerability, and exposure data. A probabilistic seismic hazard model is adopted considering a large number of seismic area sources in Nepal. Fundamental exposure data such as type of existing buildings, population, and district-wise distributions of building typologies are estimated from the 2011 national census. The fragility functions used by the National Society for Earthquake Technology (NSET) are adopted for adobe (A), brick/stone buildings with mud mortar (BM/SM), brick/stone buildings with cement mortar (BC/SC), and wooden buildings (W), while recently developed fragility functions are used for the reinforced concrete (RC) building typologies (Chaulagain et al. 2015). A set of fragility functions for each building type is converted into vulnerability functions through consequence models. In this process, the percentage of buildings in each damage state is computed at each intensity level, and multiplied by the respective damage ratio, obtaining in this manner a loss ratio for each level of ground shaking.

2 Seismic risk assessments in Nepal

In this section, the probabilistic seismic hazard analysis (PSHA) model and the selection of ground motion prediction equations in Nepal are discussed. A brief discussion on an exposure model, fragility functions, consequence models, and structural vulnerability are also presented. Moreover, the effect of local site conditions on seismic hazard and loss estimation are addressed.

2.1 Seismic hazard analysis

Earthquake disaster occurs mainly due to collapse of structures triggered by ground shaking. The most effective way to reduce earthquake disaster is to estimate the seismic hazard and disseminate this information for use in improved building design and construction. It is, therefore, important to predict ground-shaking levels in order to determine appropriate building code provisions for earthquake-resistant design of structures. Seismic hazard in the context of engineering design is generally defined as the predicted level of ground acceleration which would be exceeded with a 10 % probability at the site under consideration, owing to the occurrence of an earthquake anywhere in the region, in the next 50 years.

In fact, seismic hazard analysis is the process of evaluating the design motion of the ground during earthquakes. Scenario and probabilistic seismic hazard approaches are used for seismic hazard analysis purposes. A scenario hazard analysis involves a particular seismic event, and thus, it does not use the condition of likelihood of maximum possible ground motion. The ground motion parameters obtained by using a scenario approach of seismic hazard analysis are generally of maximum value, which is rarely used as a seismic input in the analysis of structures. However, in probabilistic seismic hazard analysis, uncertainties in earthquake size, location, and time of occurrence can be considered. Probability of exceedance of some particular value of ground motion parameter (peak ground acceleration/spectral acceleration) is calculated from the attenuation relationships. The application of an appropriate probability method is made from the available seismological and geological data. A complete study is made on selection of the appropriate attenuation and empirical relationships to estimate the ground motion parameter and to compute peak ground acceleration and response spectra. Thus, seismic hazard assessment involves a large spectrum of complex scientific assumptions and analytical modeling. A computational scheme involves (a) identification and characteristics of seismic sources; (b) evaluation of the regional seismicity; (c) use of predictive relationship to find ground motion parameter for any possible size of earthquake; and (d) combination of probability of earthquake location, size, and ground motion parameter to find total probability of exceeding a specified level of ground motion (Kramer 1996). Although these steps are region specific, a certain standardization of the approaches is essential so that reasonably comparable estimates of seismic hazard can be made worldwide, which are consistent across the regional boundaries.

2.1.1 Selection of ground motion prediction equations

Ground motion prediction equations play an important role in seismic hazard assessment for any region. Ground motion attenuation models have the strong influence on seismic hazard as well as the seismic risk (Crowley et al. 2005). The selection of ground motion models is based on the seismotectonic region, distance and magnitude applicability, period range (for spectral ordinates), ability to model site effects, and region wave propagation characteristics, among others (Silva et al. 2014a). Ground motion attenuation relations can generally be categorized into four main groups: (a) stable continental regions; (b) subduction zones; (c) active shallow crustal regions; and (d) volcanic regions. Active shallow crustal regions are characterized by active tectonics with relatively high strain rates, generally close to plate boundaries. Earthquakes occur in the upper 20–30 km of the crust, generally on well-identified mature faults (e.g., California, Italy, Turkey, Greece, and Japan). Subduction zone earthquakes are characterized by significantly different attenuation characteristics compared to shallow crustal earthquakes (Abrahamson and Silva 1997). Since the advent of plate tectonic theory, it has been recognized that subduction zones differ in many aspects relating to their geometry, geology, physics, and chemistry. The ground motion amplitudes owing to in-slab and interface types of subduction zone earthquakes are found to differ significantly. Thus, the ground motion models should address the important features of seismic source properties that characterize each tectonic regime. Youngs et al. (1997) developed separate attenuation relations for the ground motion as a result of in-slab and interface earthquakes, using a global database of about 350 horizontal components. Atkinson and Boore (2003) updated these relationships, using a larger worldwide database of about 1200 horizontal components. Atkinson and Boore relation is based on the assumption that there are no detectable differences between ground motions in different regions of the world, for the same earthquake magnitude and distance. Therefore, the applicability of this model to individual areas needs to be evaluated on a case-by-case basis. The major tectonic regions and corresponding ground motion prediction equations are summarized in Table 1. This selection is based on the recommendations of Douglas et al. (2012) and Steward et al. (2015).

Owing to the lack of strong motion data in Nepal from which an attenuation relationship could be derived, the limited research work performed in Nepal has been carried out using some standard ground motion prediction equations. The BECA Worley International Consultants Ltd (BECA 1994) used the Kawashima attenuation model (Kawashima et al. 1984), whereas Pandey et al. (2002) and Maskey (2005) used the attenuation relationship proposed by Youngs et al. (1997) for the seismic hazard assessment in their studies. On the other hand, Parajuli (2009) adopted the model proposed by Atkinson and Boore (2003) in his study. Thapa and Guoxin (2013) used the attenuation relationship developed by the China Earthquake Administration (CEA 2005) for western China for the probabilistic seismic hazard assessment of Nepal.

In the present study, we consider the tectonic region type as active shallow crust and subduction interface. The ground motion prediction equations suggested by Boore and Atkinson (2008), Chiou and Youngs (2008), Campbell and Bozorgnia (2008), Atkinson and Boore (2003), and Youngs et al. (1997) are used within a logic tree for seismic hazard and risk assessment.

2.1.2 Seismic source zones

The study of past earthquakes in and around the Nepal Himalaya shows that the whole area is seismically active. However, the microseismicity activities are particularly intense in the eastern, central, and far-western region (Pandy et al. 1999). In this regard, it is believed that stress accumulation is ongoing in the form of strain at the front of the Himalaya associated with continuous creep at depth beneath the north of the Himalaya. Figure 2 shows the spatial distribution of earthquakes in Nepal and the surrounding regions. The roughly east–west distribution of seismicity shows that the vast majority of earthquakes are located near the Main Central Thrust (MCT) in Nepal. Considering the distribution of earthquakes, fault information, and tectonic features, Pandey et al. (2002) divided the whole region of Nepal

Table 1 List of ground motion prediction equations proposed for various tectonic regimes by Douglas et al. (2012) and Steward et al. (2015)

Stable continental region	Raghu Kanth and Iyengar (2006, 2007): Peninsular India
	Douglas et al. (2006): Hybrid model for southern Norway
	Silva et al. (2002): Stochastic model for eastern North America
	Campbell (2003): Hybrid model for eastern North America
Subduction zone	BC Hydro Model, Abrahamson et al. (2012): Worldwide
	Atkinson and Boore (2003): Worldwide
	Lin and Lee (2008): Taiwan
	Youngs et al. (1997): Worldwide
Active shallow crustal regions	Abrahamson and Silva (2008): NGA model using worldwide data
	Atkinson and Boore (2011): NGA model using worldwide data
	Campbell and Bozorgnia (2008): NGA model using worldwide data
	Chiou and Youngs (2008): NGA model using worldwide data
	Zhao et al. (2006): Model using mainly Japanese data

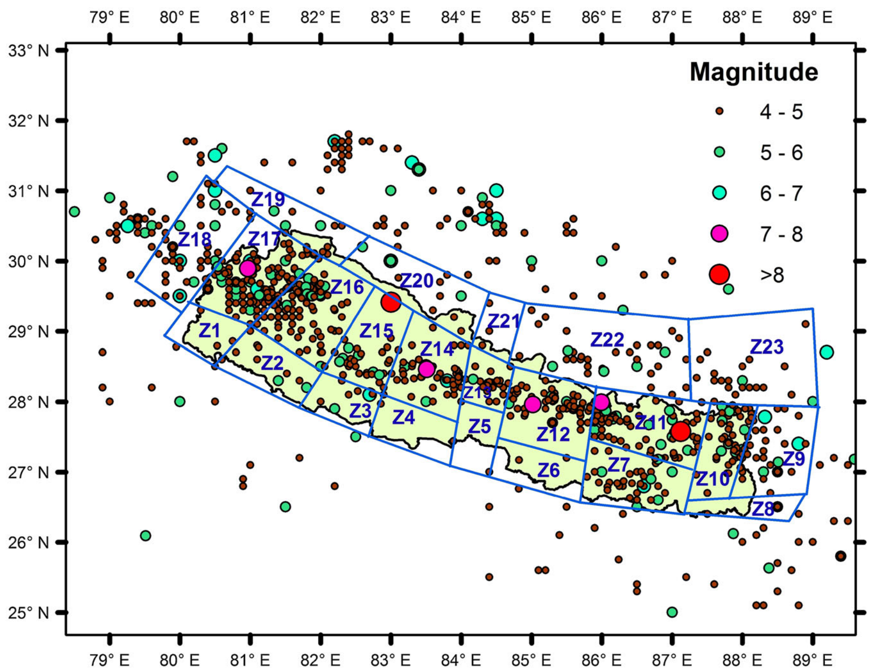

Fig. 2 Seismic source zones and spatial distribution of earthquakes in and around Nepal (Thapa and Guoxin 2013)

into ten area sources and twenty-four linear sources, of approximately 40 km each in length for probabilistic seismic hazard assessment. Their work is limited to peak ground acceleration on bedrock. However, Thapa and Guoxin (2013) divided the region in and around Nepal into twenty-three seismic source zones in their work. In the study presented herein, the same twenty-three seismic source zones are applied for the probabilistic seismic hazard analysis of Nepal.

The delineated twenty-three seismic source zones are shown in Fig. 2, and each one is considered to be seismically homogenous, so that every point within them is assumed to have an equal possibility of occurrence of an earthquake in the future. These twenty-three seismic source zones differ from one another in dimensions and hazard parameters. The historical earthquake events and the maximum magnitude of earthquakes considered in the selected seismic zones are presented in Table 2.

The earthquake catalogue of Nepal (www.seismonepal.gov.np) for the period of 1255–2011 suggests that the database before 1964 is inadequate to delineate earthquakes with a magnitude below 4 (Parajuli 2009; Thapa and Guoxin 2013). The database is more complete from 1964, when many earthquake records become available from modern seismic instruments. Pandey et al. (2002) calculated the annual rate of exceedance, *b* value, used in the Guttenberg and Richter's law in the range of 0.75–0.95, for magnitude range of 2.0–5.5. Parajuli (2009) determined *b* value of 0.76 in his study. Thapa and Guoxin (2013) estimated a *b* value of 0.85 in their study. The same *b* value of 0.85 proposed by Thapa and Guoxin (2013) is used in the present study.

Table 2 Seismic sources and historical events (Thapa and Guoxin 2013)

Seismic source zone	Historical characteristics of the area source	Maximum magnitude (M_w)
Z1	No records of strong earthquakes	6.5
Z2	No records of strong earthquakes	6.5
Z3	Magnitude (M_w) 6.2 earthquake in 1969	6.5
Z4	No records of strong earthquakes, MBT and MFT pass closely	6.5
Z5	No records of strong earthquakes	6.5
Z6	Associated with MFT, 6.3 magnitude (M_w) earthquake in 1833	6.5
Z7	Closely situated with MFT, MBT, and MCT; damaging event in 1988 ($M_w = 6.8$)	7
Z8	No records of strong earthquakes	6.5
Z9	High-level seismicity, strong earthquakes ($M_s = 6.3$, 1849; $M_s = 7.0$, 1852; and $M_s = 6.1$, 1980) during the past 200 years	8
Z10	High-level seismicity, produced two strong earthquakes ($M_s = 6.1$, 1965; and $M_s = 6.8$, 2011	8.5
Z11	Frequent earthquakes, generated two strong earthquakes with magnitudes exceeding 7.5 ($M_w = 7.6$, 1833; and $M_w = 8.2$, 1934) during the past 200 years	8.5
Z12	Situated with STDS, MCT, and MBT, experienced four major earthquakes ($M_s = 7.6$, 1255; $M_s = 7.6$, 1408; $M_s = 7.6$, 1681; and $M_s = 7.6$, 1810)	8
Z13	Related to STDS and MCT and has only produced moderate earthquakes	7.5
Z14	Frequent earthquakes, experienced two strong earthquakes ($M_w = 7$, 1936; and $M_w = 6.7$, 1954) during the past 100 years	8.5
Z15	Occupies some parts of MCT and STDS, great earthquake in 1505 ($M_s = 8.1$)	8.5
Z16	Related to the MCT and western segment of the STDS, generate strong earthquakes	8.5
Z17	Strong earthquakes	8.5
Z18	Frequent earthquakes, struck by five strong earthquakes ($M_s = 6.7$, 1911; $M_s = 6$, 1926; $M_s = 6$, 1935; $M_s = 6.5$, 1945; and $M_s = 6.3$, 1958) within the past 100 years	8
Z19	No records of strong ground motion	6.5
Z20	Strong earthquake in 1913 ($M_s = 6.2$)	6.5
Z21	Seismically less active, no strong earthquake record	6.5
Z22	Moderate earthquakes	6.5
Z23	Moderate earthquakes ($M_w = 6.4$, in 1993)	6.5

2.2 Exposure model

The development of an exposure model for seismic risk assessment at a national scale might be a very challenging task. Information about the location and classification of the existing structures can be achieved through the use of census data (e.g., Erdik et al. 2003 (Turkey); Crowley et al. 2008 (Italy); Silva et al. 2014a (Portugal)), or using other datasets to approximate building distribution, such as population datasets (Jaiswal and Wald 2010).

In this research work, the 2011 Building Census data at the district level is used as the main component for the development of exposure model.

2.2.1 Characteristics of the building stock

Nepal is located in the Himalayas, and bordered to the north by China and by India to the south, east, and west. Geographically, Nepal can be divided into three main regions: the Himalaya to the north; the middle hills consisting of the Mahabharat range and the Churia hills; and the Terai to the south. The Himalaya and its foothills make up to the northern border of the country and represent 15 % of the total land area. This is the least inhabited region of Nepal, with <7 % of the population living there. The middle hills cover about 68 % of the total land area and are home to around 43 % of the country's population. This area is the home of the ancient ethnic hill people of Nepal. The Terai is the southern part of country and is an extension of the Gangetic plains of India. It covers 17 % of the total land area. Today, about 50 % of the population occupies this region. There is a rich diversity of building structures in Nepal, resulting from its geography, ethnic group history, intensity of economic growth, and availability of local building material.

The level of building damage depends on the intensity of ground shaking and seismic performance of the structures. Therefore, a classification of the buildings is conducted as a fundamental step in estimating damage/loss. In this work, the national census data from 2011 for buildings is considered, thus disregarding public infrastructure and exclusively commercial or industrial structures. According to the census survey of 2011, the total number of individual households in the country was 5,423,297. The Terai region hosts 50.27 % of the total population, while hills and mountains comprise 43 and 6.73 %, respectively. The distribution of the buildings in Nepal is also similar to the distribution of the population (see Fig. 3). The data obtained from the National Population and Housing Census (CBS 2012) indicates that mud-bonded brick/stone buildings are more common in Nepal in all the geographical regions, comprising about 44.21 % of the building stock. In the rural region of Terai, wooden buildings are quite popular, comprising about 24.90 % of the building portfolio. Cement-bonded bricks/stones and reinforced concrete buildings have a higher representation in urban areas in most of the Terai region, Kathmandu Valley and some urban areas in the mountainous region of Nepal, constituting 17.57 and 9.94 %

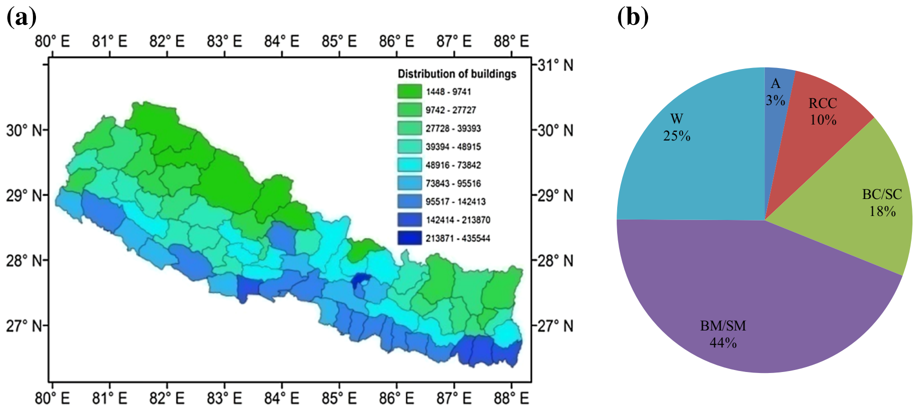

Fig. 3 **a** District-wise distribution of buildings and **b** building types in Nepal (CBS 2012)

of the building stock, respectively. The rest of the buildings have been categorized as ‘Others’. For the sake of simplicity, buildings classified as mixed, others, and not stated in national census survey have been included within the adobe category, since a similar seismic vulnerability is expected. For reinforced concrete buildings, four sub-categories have been defined: (1) current construction practices (CCP), (2) structures according to Nepal building code (NBC), (3) structures according to the modified Nepal building code (NBC+), and (4) well-designed structures (Chaulagain et al. 2013). The amount of CCP, NBC, NBC+, and WDS structures are considered as 76, 8, 8, and 8 %, respectively (Dixit 2004; Shrestha and Dixit 2008). The percentage of each building typology at a national level is described in Table 3.

For the purpose of computing the seismic hazard for each asset, it is assumed that all of the buildings are equally distributed throughout the whole district, which is a common assumption when performing seismic risk assessment on a large scale (e.g., Bommer et al. 2002; Crowley et al. 2008; Silva et al. 2014a).

2.2.2 *Estimation of economic value*

In this study, the building cost is established as the required monetary value to construct a building with the same characteristics according to present costs, herein termed as the replacement/construction cost. This value naturally depends on the location, types, and total area of the building structure. There is a lack of standard construction cost in various locations in Nepal, so the construction cost for each building type is assumed to be constant at all the districts. Table 4 presents the construction type, area per building type, and corresponding construction cost.

2.3 Structural vulnerability model

The concerns over the seismic risk in Nepal are driven not only by the high rate of seismicity but also by the extreme vulnerability of structures and infrastructures. The percentage of building construction that could be considered to be earthquake resistant is negligible, whereas the overwhelming majority of buildings and structures indicate a high vulnerability (Chaulagain et al. 2013). The seismic loss estimation is done using a vulnerability model, which describes the probability distribution of loss ratio for a set of intensity measure levels. In this study, fragility functions used by NSET are adopted for

Table 3 Vulnerability classes for the Nepalese building stock (CBS 2012)

Construction type	Vulnerability Class	Percent of buildings
Adobe	A	3.38
Brick/stone with mud mortar	BM/SM	44.21
Brick/stone with cement mortar	BC/SC	17.57
Reinforced concrete	CCP	7.54
Reinforced concrete	NBC	0.80
Reinforced concrete	NBC+	0.80
Reinforced concrete	WDS	0.80
Wooden	W	24.90

Table 4 Area and corresponding construction cost of existing Nepalese building stock

Construction type	Area per building (m^2)	Construction cost (€/m^2)
A	60	150
BM/SM	70	225
BC/SC	80	275
CCP	80	300
NBC	80	325
NBC+	80	350
WDS	90	375
W	60	200

adobe, brick/stone buildings with mud mortar, brick/stone buildings with cement mortar, and wooden buildings, while new fragility functions are used for reinforced concrete buildings (Chaulagain et al. 2015).

A single fragility function was developed during the formulation of Nepal National Building Code for seismic risk assessment in Nepal (BCDP 1994). However, this single fragility function (damage level vs ground acceleration) defining the potential damage did not differentiate different damage states at given of level of shaking. Due to this situation, Guragain (2011) modified the existing fragility functions of Nepalese buildings considering different damage states in the structure.

To this end, fragility functions for adobe and unreinforced masonry buildings in Nepal were developed using extreme loading for structures. The obtained analytical results have a good agreement with the experimental ones. For this, 17 cases of buildings with different configuration, material strength, number of stories, and mortar types were subjected to numerical simulations to calculate the probability of exceeding a number of damage states. The numerical analyses were performed at nine different levels of PGA starting from 0.05 to 1.0 g (Guragain 2011; Guragain and Dixit 2012).

The structural models for RC buildings are created considering the geometrical and material properties of Nepalese RC buildings (Chaulagain et al. 2013). The SPO2IDA framework developed by Vamvatsikos and Cornell (2006) was employed to convert static pushover curves into incremental dynamic analysis. SPO2IDA represents a tool that is capable of recreating the seismic behavior of oscillators with complex multi-linear backbones at almost any period. It provides a direct connection between the static pushover

Table 5 The mean (μ) and standard deviation (σ) per damage state for each building typology, in terms of spectral acceleration at the yielding period (Ty) (Chaulagain et al. 2015)

Building typology	T (s)	Moderate damage		Extensive damage		Collapse	
		μ	σ	μ	σ	μ	σ
CCP	0.38	0.25	0.13	0.71	0.17	1.22	0.27
NBC	0.32	0.35	0.17	0.85	0.20	1.35	0.32
NBC+	0.25	0.45	0.17	1.00	0.35	1.57	0.32
WDS	0.21	0.57	0.20	1.33	0.30	1.73	0.38

curve and the results of incremental dynamic analysis, a computer-intensive procedure that offers thorough (demand and capacity) prediction by using a series of nonlinear dynamic analyses under a suitably scaled suite of ground motion records. The results of the analysis are summarized into their 16, 50, and 84 % fractile IDA curves. It offers effectively instantaneous estimation of demands and limit-state capacities, in addition to conventional strength reduction R-factor and inelastic displacement ratios, for any SDOF whose SPO curve can be approximated by a quadrilinear backbone. The mean (μ) and standard deviation (σ) per damage state for each building typology are presented in Tables 5 and 6.

2.3.1 *Consequence model employed to convert fragility curves into vulnerability curves*

Vulnerability functions can be derived from fragility functions using consequence models, which describe the percentage of financial loss for a given level of performance or damage state (Silva et al. 2014b). The consequence models developed for Italy, Greece, Turkey, California, and Portugal are different. All these models have different damage scales, and each damage ratio is influenced by the damage level in the structure. In this study, each set of fragility functions is converted into a vulnerability function, through the employment of a consequence model. In this process, the percentage of buildings in each damage state is computed at each intensity measure level and multiplied by the respective damage ratio, thus obtaining a loss ratio for each level of peak ground acceleration or spectral acceleration. The consequence model used in the development of the vulnerability model for the Nepalese building stock is presented in Table 7.

2.4 Local site effects

Site conditions play a major role in establishing the damage potential of incoming seismic waves from major earthquakes. In the 1985 Michoacan ($M_s = 8.1$) earthquake, only moderate damage was reported in the vicinity of the epicenter, while in Mexico City, located 350 km away, extensive damage was observed (Kramer 1996). In this earthquake, the bedrock outcrop motions were amplified about five times. In the 1989 Loma Prieta earthquake, major damage occurred on soft soil sites in the San Francisco–Oakland region, where the spectral accelerations were amplified two to four times over adjacent rock sites (Housner 1989) and caused severe damage. It shows that surface-level peak ground acceleration and spectral acceleration values can be different from bedrock values, depending on local soil conditions. In fact, shaking is stronger where the shear wave velocity is lower.

Table 6 The mean (μ) and standard deviation (σ) per damage state for each building typology, in terms of peak ground acceleration

Building typology	Moderate damage		Extensive damage		Collapse	
	μ	σ	μ	σ	μ	σ
Adobe	−3.22	0.65	−1.99	0.77	−1.45	0.64
BM	−2.14	0.72	−1.66	0.72	−1.05	0.66
BC	−1.82	0.68	−1.06	0.67	−0.62	0.72
W	−1.08	0.64	−0.39	0.64	0.00	0.64

Table 7 Consequence model used in the development of the vulnerability model for the Nepalese building stock

Damage state	Damage ratio
Moderate damage	0.30
Extensive Damage	0.60
Collapse	1.00

Amplification of amplitudes of soil particle motion from vertically propagating shear waves occurring from bedrock depends on the type and geotechnical properties of overburdening soil. The soil type, pore water pressure, and the level of the water table are other significant site parameters.

The use of the average velocity of seismic shear waves in the top 30-m layer (Vs30) has become a very common standard to characterize seismic site conditions. The United States design code (BSSC 2001) specifically requires this measurement to represent the local site conditions. Similarly, the European design regulation (EC8—CEN 2004) also provides soil classification using this parameter. Moreover, many ground motion prediction equations (e.g., Atkinson and Boore 2006; Chiou and Youngs 2008), which are fundamental for seismic hazard and risk assessment, have been calibrated against seismic station site conditions, described with Vs30 values (Wald and Allen 2007).

In this study, the OpenQuake-engine (Silva et al. 2014c) uses ground motion prediction equations that require the definition of a Vs30 value for each location where the seismic hazard and risk are going to be computed. If such parameter is not available at a given location, the OpenQuake-engine uses the closest Vs30 value. The site effect in the present

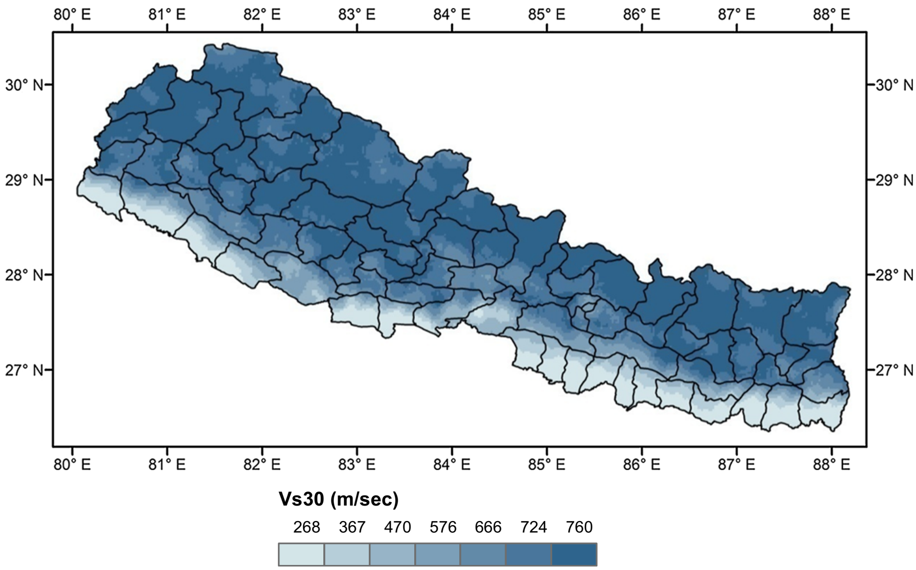

Fig. 4 Vs30 map of Nepal (http://www.usgs.gov)

study is considered using the Vs30 map downloaded from the USGS Vs30 database. The spatial distribution of Vs30 values is presented in Fig. 4.

3 Results

3.1 Seismic hazard

Probabilistic seismic hazard has been estimated in this study. As presented in Fig. 5, the estimated peak ground acceleration value (PGA in g) at 10, 5, 2, and 1 % probability of exceedance in 50 years is in the range of 0.22–0.50, 0.30–0.64, 0.42–0.85, and 0.51–1.07 g, respectively. In all the cases, the highest ground motions are observed in eastern parts and the mid-western region of the country, and lower values are observed in the southern Nepal.

The estimated values are consistent with some recent studies, about 0.50 g for 10 % probability of exceedance in 50 years in far-western Nepal obtained by Mahajan et al. (2010). Nath and Thingbaijam (2012) obtained peak ground acceleration values of 0.35–0.40 and 0.70–0.80 g for 10 and 2 % probability of exceedance in 50 years in eastern Nepal, respectively. However, the value is in the range of 0.70–0.80 g for 2 % probability of exceedance in 50 years in far-western Nepal. The obtained results are also similar to the values obtained by Bhattarai (2010), where PGA at rock and soil sites in the order of 0.29 and 0.39 g was estimated in eastern Nepal, both for 10 % probability of exceedance in 50 years. Pandey et al. (2002) estimated up to 0.50 g peak ground acceleration value in bedrock for 10 % probability of exceedance in 50 years. Parajuli (2009) estimated the peak ground acceleration corresponding to 40, 10, and 5 % probability of exceedances in 50 years. The result showed that eastern and far-western regions may experience bigger

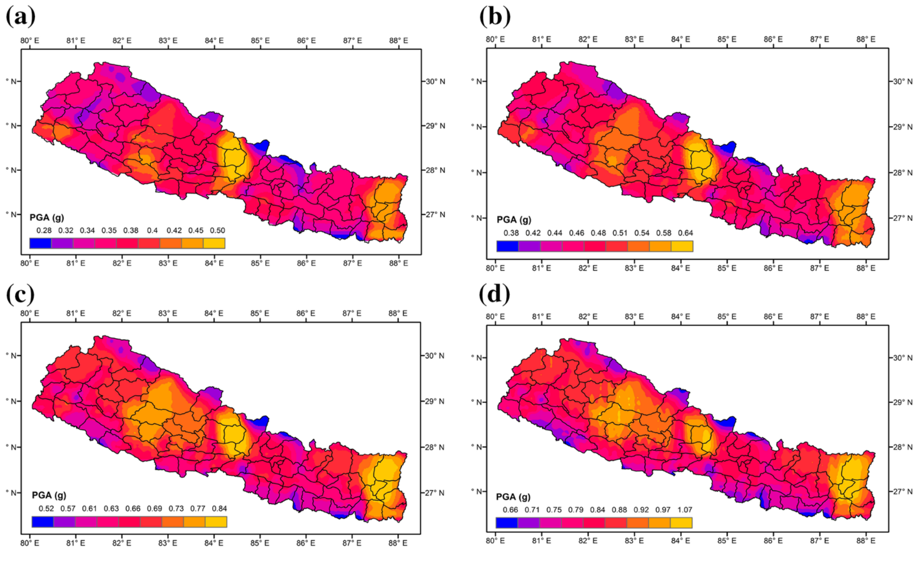

Fig. 5 Seismic hazard maps of Nepal showing the peak ground acceleration distribution with: **a** 10 % probability of exceedance in 50 years, **b** 5 % probability of exceedance in 50 years, **c** 2 % probability of exceedance in 50 years, and **d** 1 % probability of exceedance in 50 year

peak ground accelerations than in central regions. Moreover, Thapa and Guoxin (2013) calculated peak ground acceleration in bedrock with 63, 10, and 2 % probability of exceedance in 50 years. The estimated PGA values are in the range of 0.07–0.16, 0.21–0.62, and 0.38–1.10 g for 63, 10, and 2 % probability of exceedance in 50 years, respectively.

3.2 Uniform hazard spectra

Traditionally, PGA has been used to characterize ground motion. However, in recent years, the preferred parameter has been the spectral acceleration (S_a) for the fundamental period of vibration. For finding uniform hazard spectra (UHS), seismic hazard curves of spectral acceleration are computed for a range of frequency values. From these hazard curves, response spectra for a specified probability of exceedance over the entire frequency range of interest are obtained. The uniform hazard spectra with 10, 5, 2, and 1 % probability of

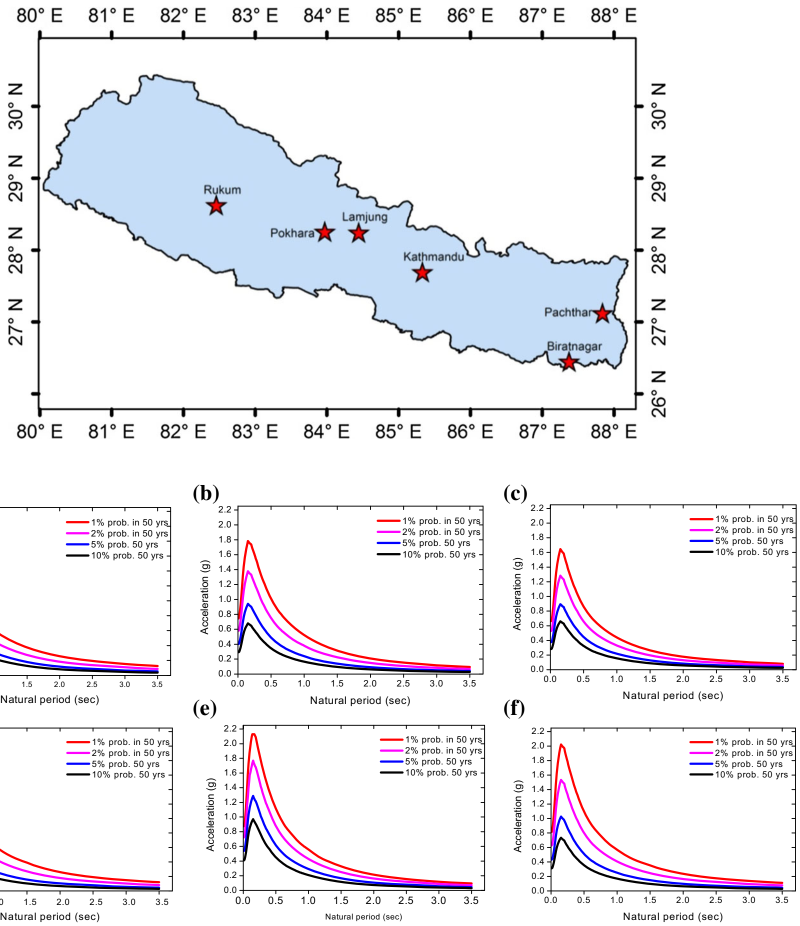

Fig. 6 Uniform hazard spectra in 5 % damping at different locations in Nepal: **a** Biratnagar sub-metropolitan city, **b** Kathmandu metropolitan city, **c** Pokhara sub-metropolitan city, **d** Panchthar, **e** Lamjung, and **f** Rukum district

exceedance of earthquakes in 50 years for six different places in Nepal is plotted in Fig. 6. It indicates that the values are higher in mountainous districts. The maximum spectral acceleration for Biratnagar, Kathmandu, and Pokhara sub-metropolitan city are 0.70, 0.67, and 0.66 g, respectively, occurring for 475 years return period. In Lamjung district, the spectral acceleration for 10 % probability of exceedance in 50 year is 0.97 g, which is around 40 % higher than the Kathmandu, Biratnagar, and Pokhara sub-metropolitan city. The expected spectral acceleration value in Kathmandu for the 2475 years return period is 1.38 g. These results are similar to the values proposed by Bhattarai (2010).

3.3 Seismic risk

Using the set of loss exceedance curves for each asset, a mean loss map for 10, 5, 2, and 1 % probability of exceedance in 50 years is computed and presented in Fig. 7. The estimated economic losses in Nepal are mostly concentrated in the Kathmandu Valley and southeast region of Nepal. Despite the moderate seismic hazard in the Kathmandu Valley and southeast region, significant economic losses are still expected, owing to the presence of large number of brick and stone buildings in medium-to-soft soils. As for example in soft soil, spectral acceleration can be amplified by a factor of 1.5 for short periods and by 2.0 for longer periods (Steward et al. 2015). In the Kathmandu Valley, the losses are 8.3, 8.2, 7.6, and 6.7 billion euro, respectively, which is around 15 % of the total economic value in the whole country. The disaggregation of the economic losses according to the building typology indicates that the brick and stone masonry buildings are responsible for more than 50 % of the losses, which is a predictable scenario considering the large proportion of this type of construction in Nepal (44.21 %), associated with its high seismic vulnerability.

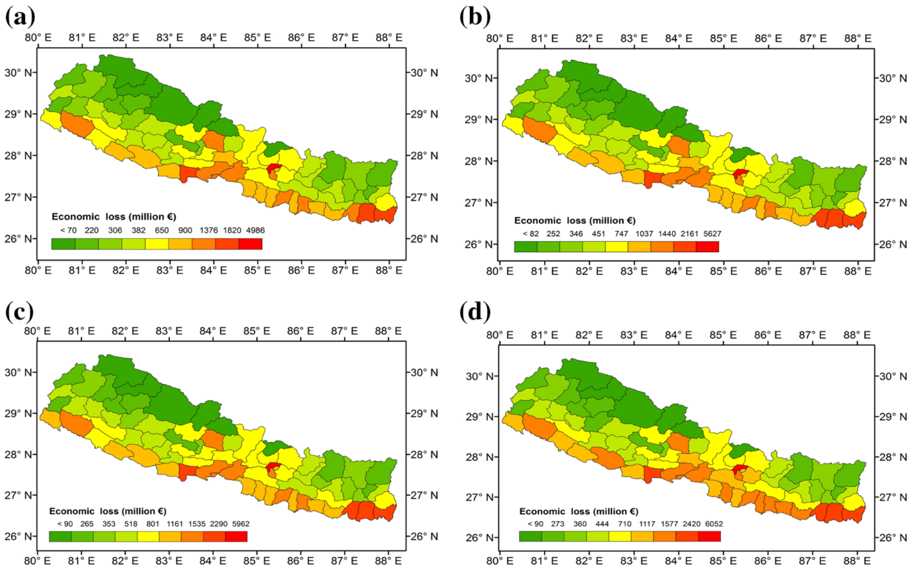

Fig. 7 Economic loss map of Nepal: **a** with 10 % probability of exceedance in 50 years, **b** with 5 % probability of exceedance in 50 years, **c** with 2 % probability of exceedance in 50 years, and **d** with 1 % probability of exceedance in 50 years

3.4 Earthquake loss estimation for historical earthquake scenario

The distribution of building damage and corresponding economic losses due to the recurrence of the 1934 Bihar–Nepal (8.2 M_w) earthquake is presented in this section. The scenario epicenter was assumed in the same location as that of the 1934 earthquake. The damage pattern of each building typology is determined using OpenQuake-engine which is capable of estimating the distribution of buildings in each damage state due to the occurrence of a single event (Silva et al. 2014c). The estimated damage pattern of each building typology in Nepal is tabulated in Table 8.

As presented in Fig. 8, it can be seen that about 22 % of adobe, 9 % of BM/SM, 7 % of BC/SC, and 8 % of CCP buildings would collapse due to the recurrence of the 1934 scenario earthquake. The collapse would be limited to 7, 5, 2, and 2 % for NBC, NBC+, WDS, and W buildings, respectively. The result also indicates that about 282,450 masonry buildings would collapse due to the recurrence of 1934 scenario earthquake, which follows the similar trends of Kashmir ($M_w = 7.6$; 2005) and Java ($M_w = 6.3$; 2006) earthquakes (Meguro 2008).

The structural and financial loss due to the 1934 scenario earthquake are mostly concentrated in the eastern half of the Nepal (see Fig. 9). The total financial loss is about 13 billion euro, which is about 70 % of Nepalese gross domestic product (GDP) in 2013. The economic loss in the Kathmandu Valley is about 2.5 billion euro which is about 20 % of the total loss.

4 Conclusions and recommendations

This study estimates the higher seismic hazard in the mid-western and eastern parts of Nepal, whereas the southern Nepal has the lowest seismic hazard. The expected peak ground acceleration at 10, 5, 2, and 1 % probability of exceedance in 50 years is in the range of 0.22–0.50, 0.30–0.64, 0.42–0.85, and 0.51–1.07 g, respectively. Similarly, the results also indicate that Biratnagar sub-metropolitan city, Kathmandu metropolitan city, and Pokhara sub-metropolitan city have spectral acceleration of 0.70, 0.67, and 0.66 g, respectively (for 475 years returns periods).

Table 8 Damage states of buildings in Nepal

Buildings	No damage	Moderate damage	Extensive damage	Collapse
A	44,160	55,200	44,160	40,480
BM/SM	1198,720	599,360	383,591	215,770
BC/SC	609,729	171,486	104,797	66,689
CCP	208,917	94,218	73,736	32,771
NBC	25,009	8193	6899	3018
NBC+	27,165	8193	5605	2156
WDS	31,046	5174	6037	862
W	891,100	310,535	121,514	27,003
Total	3035,846	1252,358	746,338	388,750

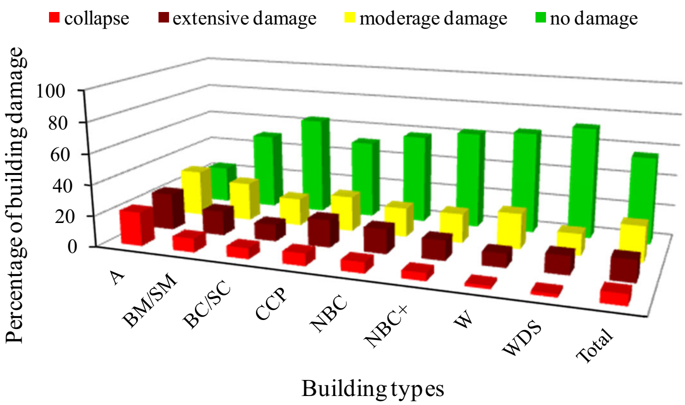

Fig. 8 Building damages due to earthquake scenario in Nepal

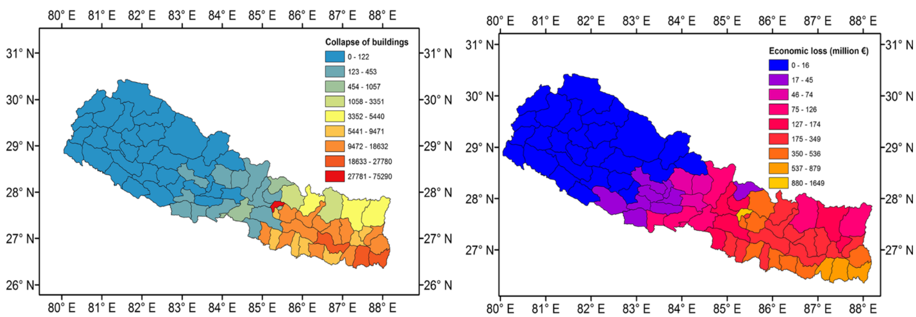

Fig. 9 Total building collapse map and economic loss map due to the repetition of the 1934 historical event

About 22 % of adobe, 9 % of BM/SM, 7 % of BC/SC, and 8 % of CCP buildings would be collapsed resulting from the recurrence of 1934 scenario earthquake. From these results, it can be seen that about 14 % of the buildings would experience the extensive damage, whereas the overall collapse of building would be limited to 7 % only. The trends of building damage indicate that the brick and stone masonry buildings are liable for more than 50 % of the losses, which is a predictable scenario considering the large proportion of seismically vulnerable construction in Nepal. The total economic loss would be about 13 billion euro, which is about 70 % of Nepalese gross domestic product (GDP) in 2013. The results are similar to the earthquakes of Haiti (2010), Guatemala (1976), Nicaragua (1972), and El Salvador (1986) that caused economic losses of approximately 120, 98, 82, and 40 % of the normal gross domestic product (GDP) of each country, respectively (Daniell et al. 2010). All the structural and financial losses of the building structures are mostly concentrated in the eastern half of Nepal.

The results of this study are useful for national state, local governments, decision makers, engineers, planners, emergency response organizations, builders, universities, and the general public, who require seismic hazard and risk estimates for land-use planning, improved building design and construction, emergency response preparedness plans, economic forecasts, housing and employment decisions, and many other types of risk mitigation.

Acknowledgments This research investigation is supported by the Eurasian University Network for International Cooperation in Earthquake (EU-NICE), through a fellowship for Ph.D. research of the first author. This support is gratefully acknowledged.

References

Abrahamson NA, Silva W (1997) Empirical response spectral attenuation relations for shallow crustal earthquakes. Seismol Res Lett 68:94–127

Abrahamson NA, Silva W (2008) Summary of the Abrahamson & Silva NGA ground-motion relations. Earthq Spectra 24(1):67–97

Abrahamson N, Gregor N, Addo K (2012) BC Hydro ground motion prediction equations for subduction earthquakes. Earthq Spectra

Atkinson GM, Boore DM (2003) Empirical ground-motion relations for subduction zone earthquakes and their application to Cascadia and other regions. Bull Seismol Soc Am 93(4):1703–1729

Atkinson GM, Boore DM (2006) Earthquake ground-motion prediction equations for eastern North America. Bull Seismol Soc Am 96(6):2181–2205

Atkinson GM, Boore DM (2011) Modifications to existing ground-motion prediction equations in light of new data. Bull Seismol Soc Am 101(3):1121–1135

BECA Worly International (New Zealand) in association with SILT Consultants (P.) Ltd. (Nepal), TAEC Consult (P.) Ltd. (Nepal), Golder Associates (Canada), Urban Regional Research (USA) (1994) Seismic hazard mapping and risk assessment for Nepal. GoN/UNDP/UNCHS (Habitat), Subproject 88/054/21.03, Kathmandu, Nepal

Bhattarai GK (2010) Probabilistic seismic hazard assessment and ground response analysis of Biratnagar sub-metropolitan city, Eastern Nepal. ME Thesis, Purbanchal University, Nepal

Bommer JJ, Spence R, Erdik M, Tabuchi S, Aydinoglu N, Booth E, Re DD, Pterken D (2002) Development of an earthquake model for Turkish catastrophe insurance. J Seismol 6:43–116

Boore DM, Atkinson GM (2008) Ground-motion prediction equations for the average horizontal component of PGA, PGV, and 5%-damped PSA at spectral periods between 0.01 and 10.0s. Earthq Spectra 24(1):99–138

BSSC (Building Seismic Safety Council) (2001) NEHRP Recommended Provisions for Seismic Regulations for New Buildings, and Other Structures, 2000 ed. Part 1: Provisions. Building Seismic Safety Council for the Federal Emergency Management Agency (Report FEMA368), Washington, DC, USA

Building Code Development Project (BCDP) (1994) Seismic hazard mapping and risk assessment for Nepal. GoN, Ministry of Housing and Physical Planning, Kathmandu

Campbell KW (2003) Prediction of strong ground motion using the hybrid empirical method and its use in development of ground motion (attenuation) relations in eastern North America. Bull Seismol Soc Am 93:1012–1033

Campbell KW, Bozorgnia Y (2008) NGA ground motion model for the geometric mean horizontal component of PGA, PGV, PGD and 5 % damped linear elastic response spectra for periods ranging from 0.01 to 10 s. Earthq Spectra 24(1):139–171

CEN Eurocode 8 (2004) Design of structures for earth quake resistance—Part 1: general rule, seismic actions and rule for buildings. EN 1998-1: 2004. Comite Europeen de Normalisation, Brussels

Centre Bureau of Statistics (CBS) (2012) National Report, National Planning Commission Secretariat. Central Bureau of Statistics, Kathmandu, Nepal

Chaulagain H, Rodrigues H, Jara J, Spacone E, Varum H (2013) Seismic response of current RC buildings in Nepal: a comparative analysis of different design/construction. Eng Struct 49:284–294

Chaulagain H, Rodrigues H, Silva V, Spacone E, Varum H (2015) Earthquake loss estimation for the Kathmandu Valley. Bull Earthq Eng (in review)

China Earthquake Administration (CEA) (2005) Training material on seismic hazard analysis for Engineering Sites (GB17741-2005)

Chiou BSJ, Youngs RR (2008) An NGA model for the average horizontal component of peak ground motion and response spectra. Earthq Spectra 24(1):173–215

Crowley H, Bommer JJ, Pinho R, Bird J (2005) The impact of epistemic uncertainty on an earthquake loss model. Earthq Eng Struct Dyn 34:1653–1685

Crowley H, Borzi B, Pinho R, Colombi M, Ondida M (2008) Comparison of two mechanics-based methods for simplified structural analysis in vulnerability assessment. Adv Civ Eng 2008:19

Daniell JE, Wenzel F, Khazai B (2010) The cost of historic earthquakes today economic analysis since 1900 through the use of CATDAT. In: Proceedings of the Australian earthquake engineering society conference, Perth, Australia

Dixit A (2004) Promoting safer building construction in Nepal. Thirteen World Conference on Earthquake Engineering. Paper No: 1717

Douglas J, Bertil D, Roulle A, Dominique P, Jousset P (2006) A preliminary investigation of strong-motion data from the French Antilles. J Seismol 10(3):271–299

Douglas J, Cotton F, Alessandro C, Boore DM, Abrahamson NA, Akkar S (2012) Compilation and critical review of GMPEs for the GEM-PEER Global GMPEs Project. In: 15th world conference of earthquake engineering, Lisbon, Portugal

Erdik M, Aydinoglu N, Fahjan Y, Sesetyan K, Demircioglu M, Siyahi B, Durukal E, Ozbey C, Biro Y, Akman H, Yuzugullu O (2003) Earthquake risk assessment for Istanbul Metropolitan Area. Earthq Eng Eng Vib 2(1):1–23

Guragain R (2011) Development of fragility function for Nepalese building structure. Nepal National Building Code, 1994; modified by Guragain R, NSET, Nepal (unpublished)

Guragain R, Dixit A (2012) Development of fragility functions for low strength masonry buildings in Nepal using applied element methods. In: 15th world conference of earthquake engineering, Lisbon, Portugal

Housner GW (1989) Competing against time. Report to Governor Deukmejian of California, Governor's Board of Inquiry on the 1989 Loma Prieta Earthquake

Jaiswal K, Wald D (2010) An Empirical model for global earthquake fatality estimation. Earthq Spectra 26(4):1017–1037

JICA (2002) The study on Earthquake disaster mitigation in the Kathmandu Valley, Kingdom of Nepal. Japan International Cooperation Agency and the Ministry of Home Affairs of Nepal, vol I, II and III

Kawashima K, Aizawa K, Takahashi K (1984). Attenuation of peak ground motion and absolute acceleration response spectra. In: Proceedings of eighth world conference on earthquake engineering, vol II, pp 257–264

Kramer S (1996) Geotechnical earthquake engineering. Prince Hall, New Jersey

Lava J, Avouac JP (2000) Active folding of fluvial terraces across the Siwaliks Hills, Himalayas of central Nepal. J Geophys Res 105:5735–5770

Lin P-S, Lee C-T (2008) Ground-motion attenuation relationships for subduction-zone earthquakes in northeastern Taiwan. Bull Seismol Soc Am 98(1):220–240

Mahajan AK, Thakur VC, Sharma ML, Chauhan M (2010) Probabilistic seismic hazard map of NW Himalaya and its adjoining area, India. Nat Hazards 53:443–457

Maskey PN (2005) Selection of attenuation laws for estimation of seismic input in Nepal. J Inst Eng 5:75–85

Meguro K (2008) Technological and social approaches to achieve earthquake safer non-engineered houses. In: Proceedings of 14th world conference on earthquake engineering, Beijing, China

Nath SK, Thingbaijam S (2012) Probabilistic seismic hazard assessment of India. Seismol Res Lett 83(1):135–149

NSET (2001) The Kathmandu Valley Earthquake risk management action plan, a Product of the Kathmandu Valley Earthquake Risk Management Project

Pandey MR, Tandukar RP, Avouac JP, Lave J, Massot JP (1995) Interseismic strain accumulation on the Himalayan crustal ramp (Nepal). Geophys Res Lett 22(7):751–754

Pandey MR, Chitrakar GR, Kafle B, Sapkota SN, Rajaure SN, Gautam UP (2002) Seismic hazard map of Nepal. Department of Mines and Geology, Kathmandu

Pandy MR, Tandukar RP, Avouac JP, Vergne J, Heritier T (1999) Seismotectonics of Nepal Himalaya from local seismic network. J Asian Earth Sci 17:703–712

Parajuli HR (2009) Dynamic analyses of low strength masonry houses based on site specific earthquake ground motions. PhD Thesis, Department of Urban Management, Graduate School of Engineering, Kyoto University, Japan

Raghu Kanth STG, Iyengar RN (2006) Seismic hazard estimation for Mumbai city. Curr Sci 91(11):1486–1494

Raghu Kanth STG, Iyengar RN (2007) Estimation of seismic spectral acceleration in peninsular India. J Earth Syst Sci 116(3):199–214

Rana BJB (1935) Nepal ko Maha Bhukampa (Great earthquake of Nepal). Jorganesh Press, Kathmandu

Shrestha B, Dixit AM (2008) Standard design for earthquake resistant buildings and aid to building code implementation in Nepal. Fourteen World Conference on Earthquake Engineering

Silva WJ, Gregor N, Darragh R (2002) Development of regional hard rock attenuation relations for central and eastern North America. Technical report, Pacific Engineering and Analysis, El Cerrito

Silva V, Crowley H, Pinho R, Varum H (2014a) Seismic risk assessment for mainland Portugal. Bull Earthq Eng 13(2):429–457

Silva V, Crowley H, Pinho R, Varum H (2014b) Investigation of the characteristics of Portuguese regular moment-frame RC buildings and development of a vulnerability model. Bull Earthq Eng. doi:10.1007/s10518-014-9669-y

Silva V, Crowley H, Pagani M, Monelli D, Pinho R (2014c) Development of the OpenQuake engine, the Global Earthquake Model's open-source software for seismic risk assessment. Nat Hazards 72(3):1409–1427

Steward J, Douglas J, Boore D, Campbell K, Delavaud E, Erdik M, Stafford P (2015) Selection of a global set of ground motion prediction equations: work undertaken as part of Task 3 of the GEM-PEER Global GMPEs project. PEER Report 2012, Pacific Earthquake Research Centre

Thapa N (1988) BhadauPanchKoBhukampa (in Nepali). Central Disaster Relief Committee, Nepal

Thapa DR, Guoxin W (2013) Probabilistic seismic hazard analysis in Nepal. Earthq Eng Eng Vib 12:577–586

Upreti BN (1999) An overview of the stratigraphy and tectonics of the Nepal Himalaya. J Asian Earth Sci 17:577–606

Vamvatsikos D, Cornell CA (2006) Direct estimation of the seismic demand and capacity of oscillators with multi-linear static pushovers through IDA. Earthq Eng Struct Dyn 35:1097–1117. doi:10.1002/eqe.57

Wald D, Allen T (2007) Topographic slope as a proxy for seismic site conditions and amplification. Bull Seismol Soc Am 97:1379–1395

Wyss M (2005) Human losses expected in Himalayan Earthquakes. Nat Hazard 35:305–314

Wyss M, Nekrasova A, Kossobokov V (2012) Errors in expected human losses due to incorrect seismic hazard estimates. Nat Hazard. doi:10.1007/s11069-012-0125-5

Youngs RR, Chiou BSJ, Silva WJ, Humphrey JR (1997) Strong ground motion attenuation relationships for subduction zone earthquakes. Seismol Res Lett 68(1):58–73

Zhao JX, Zhang J, Asano A, Ohno Y, Oouchi T, Takahashi T, Ogawa H, Irikura K, Thio HK, Somerville PG, Fukushima Y, Fukushima Y (2006) Attenuation relations of strong ground motion in Japan using site classification based on predominant period. Bull Seismol Soc Am 96(3):898–913